International Journal of Engineering and Technical Research (IJETR)
ISSN: 2321-0869 (O) 2454-4698 (P), Volume-3, Issue-10, October 2015

Damage mechanism of service exposed reformer tubes in petrochemical industries-a review

Archisman Ray, Anant Raj, Bangsidhar Goswami, Ashok Kumar Ray

***Abstract*— This review article deals with damage analysis of service exposed reformer tubes where packed nickel catalysts are used for synthesis of hydrogen, ammonia etc. in petrochemical industries based on hot tensile, accelerated creep or stress rupture tests and detailed microstructural analysis for remaining life assessment and life management studies. This research has become a regular task because of large range of time for failure (3 to 15 years) compared to designed life (11.4 years or 1, 00,000 hours) and huge loss associated to damage, production and safety hazards. Utilization of appropriate inspection during plant shut down has been strategic short term life assessment. Inspection of micro-cracks, hot spot formation, carburization/metal dusting for inner wall and oxidation, tube diameter increment for outer wall inspection have been traditional symptoms of expiry of tubes after service exposure. This paper therefore aims at studying damage mechanisms of reformer tubes in response to wide time frame for failures and accidents involved, even after stipulation of designed time schedules.**

***Index Terms*— HK40 steel, HP40 steel, Reformer tube, Centrifugal castings, Cavitations, Creep, Accelerated creep, Hot tension, Catalyst, Hydrogen, Methane.**

I. INTRODUCTION

Steam reforming, auto-thermal or secondary reforming is the key technology, in today's petrochemical and fertilizer industries. Natural gas is used for production of ammonia, methanol, hydrogen, carbon monoxide etc. Catalytic chemical conversion of natural gas with steam and/or oxygen-containing gas is used in reforming reaction. Hydrocarbon feed is reacted with steam to produce synthesis gas in catalyst packed tubes. Main reactions in primary reformer tube have been as follows:

Steam reforming of higher hydrocarbons [1]:

$$C_nH_{2n+2} + nH_2O \rightarrow nCO + (2n+1)H_2,\ \Delta H>0 \qquad (1)$$

Steam reforming of methane:

$$CH_4 + H_2O \rightarrow CO + 3H_2,\ \Delta H>0 \qquad (2)$$

Water gas shift reaction:

$$CO + H_2O \rightarrow CO_2 + H_2,\ \Delta H<0 \qquad (3)$$

Archisman Ray, Final year B.Tech student in Chemical Engineering Heritage Institute of Technology, Kolkata-700107

Anant Raj, (PhD scholar under Dr. Ashok Kumar Ray) Professor of Mechanical Engineering Department, R.V.S. College of Engineering & Technology, Jamshedpur-831012, India

Dr. Bangsidhar Goswami, Asst. Professor, Department of Metallurgy, R.V.S. College of Engineering & Technology, Jamshedpur-831012, India

Dr. Ashok Kumar Ray, Professor of Academic CSIR Chief Scientist (Scientist-G) and Group Leader/Head of Materials Testing and Evaluation Section (Creep, Fatigue & Fracture) of Materials Science and Technology Division CSIR- NML (National Metallurgical Laboratory) PO-Burmamines, Jamshedpur-831007, India TF-0657-2345197(O) Mobile-9931321596

Process is highly endothermic. Under service exposure reformer tubes have been subjected to carbonization, oxidation, overheating, stress corrosion cracking, sulfidation and thermal cycling. Traditional stainless steel application for vertical reformer tube has been substituted by centrifugally cast HK40 alloys in 60's, which has been subsequently replaced by HP modified alloys in 80's. Even after these advancements, failure occurrences between 3 to 15 years range from as designed performance of 11.4 years, these alloy tubes have been subjected for inspection, assessment and reassessment of acceptable life during operations. Various standards have been considered for test of these tubes, e.g. standards of tension and impact tests have been considered according to ASTM-E8 and ASTM-E23-28 respectively. Of innumerable possibilities of analysis and interpretations for description about so large ranged performance of reformer tubes following microstructure features have been versed: These have been (a) austenite matrix, (b) carbide precipitation, these have been (1) coarse and (2) fine varieties formed by (1) primary and (2) secondary mechanisms respectively, (c) interplays of dissolution, coarsening, agglomeration, etc. of precipitates based on incidental variation in temperature, e.g. catalyst poisoning, or hot spot formation, (d) formation of grain boundary voids and coarsening of carbides causes creep cavities during elevated temperature operations [1-11].

Aim of this review has been to study damage analysis of reformer tube in response to wide time frame for failures and accidents involved, even after stipulation of designed time schedules.

II. INDUSTRIAL PERFORMANCE

Traditions of cost minimization from 1960's and better mechanical property has been achieved for components of petrochemical plant like reformer tube and pyrolysis tubes by centrifugal cast of 25Cr20Ni heat resistant alloyed steels. Advantages of these series of steels have been higher creep rupture strength and resistance to oxygen, sulpher and carbon. Improvement in mechanical properties have been accounted from (i) formation of distributed network of primary eutectic carbides at the dendrites and dendrite grain boundaries during solidification and (ii) heterogeneous precipitation of fine array of secondary carbides in dendrites and grains from as cast supersaturated solid solutions during services. Primary carbides reduce grain boundary sliding and secondary precipitations restrict dislocation motion during high temperature service. Secondary precipitates have been coarsened with life to deteriorate properties upon coalescence. Therefore primary eutectic precipitation has been more acceptable to produce long term strengthening effects at higher temperature, e.g. 1323 K. Interests to increase long term high temperature strength bearing capacity

have been developed by alloy additions. Some of these have been shown in table 1 [12].

Table 1: Chemical compositions of typical tube materials [12].

Material	Amount (wt.%) of the following elements							
	Ni	Cr	C	Nb	W	Si	Mn	Other
HK 40	20.5	24.5	0.4	---	---	1.25	1.5	Mo<0.5
Mod. HK	22.5	23.5	0.42	---	---	1.2	1.0	---
Hi-Si HK	21.5	24.1	0.5	---	---	2.2	1.5	---
HP	33.8	24.3	0.43	0.69	---	1.71	1.11	---
36×S	34.1	25.9	0.43	1.11	1.52	1.6	1.2	---
36×A	34.2	25.1	0.43	0.8	---	1.5	1.4	3.3Al
PG2535Nb	35.2	25	0.45	1.57	---	2.2	1.0	---
KHR35CW	35.4	25	0.4	1.4	1.2	1.6	0.9	0.4Mo
36× T	44.8	31.5	0.35	1.34	1.7	1.6	0.9	---
PG28485	45.7	27.7	0.57	---	4.25	1.8	1.11	---

Fabrication of reformer tubes/ pipes, e.g. with gradually increasing Ni content, additions of W, Mo, Nb, Ti and Zr is very expensive. Improvement in properties of heat-resistant tube materials used in cracking processes has led to development of tube fabrication process which involves centrifugal force and electromagnetic field. Relations between solidification conditions as per cooling rate from force of centrifuge and electro-magnetic field associated have been shown in figure 1 and table 2. Steel has been melted at 1923 K in a high frequency induction furnace and poured into rotating (e.g. 1700 rpm) mould within electromagnetic field. This is referred to as electromagnetic centrifugal casting route for production of reformer tubes. Fabricated tube and related sampling technique of X.Q.Wu et al. [12] has been shown in figure 2. Figure 3 has shown to reproduce variation in typical macrostructures based on variation in cooling rate versus electromagnetic field strength. Increase in cooling rate has increased columnar grain zone while increase in electromagnetic field has increased thickness of equiaxed zone.

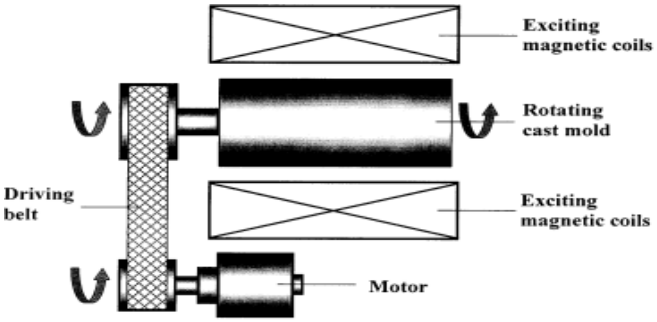

Figure 1: Schematic diagram of the electromagnetic centrifugal casting equipment [12].

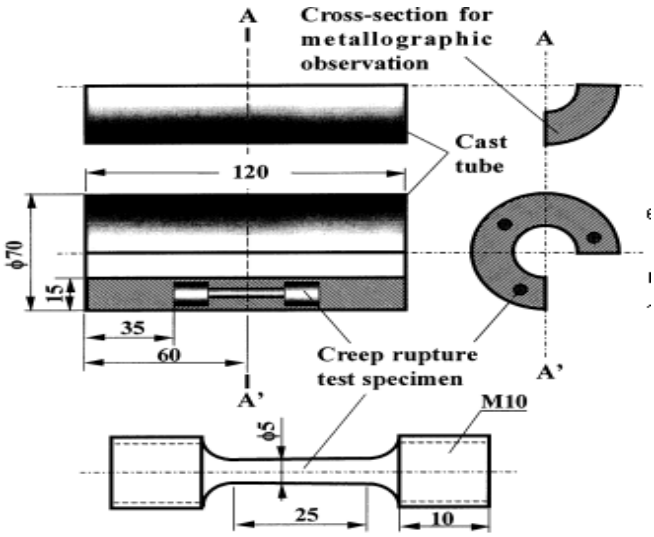

Figure 2: Sampling diagram and the sizes of the creep rupture test specimens' [12].

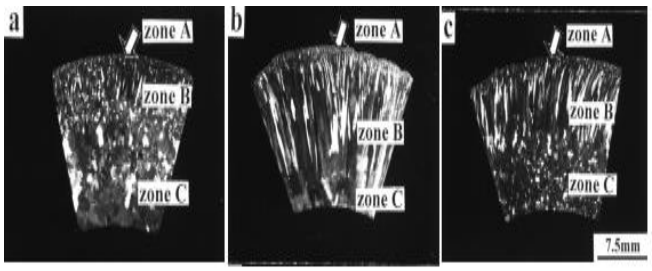

Figure 3: Macrostructures on the cross-sections of the centrifugally cast 25Cr20Ni heat-resistant steel tubes: (a) Typical centrifugal solidification, (b) centrifugal solidification with increased cooling rate and (c) centrifugal solidification with increased electromagnetic field. (zone A = chill zone, zone B = columnar grain zone and zone C = equiaxed grain zone) [12].

Table 2: Thickness fraction of macrostructures and volume fraction of eutectic carbides in cast tubes [12].

Tube	Thickness fraction (%)			Zone B			Zone C			F%
	Zone A	Zone B	Zone C	V_t%	V_{gb}%	V_{gb}/V_t	V_t%	V_{gb}%	V_{gb}/V_t	
C0	4	27	69	6.54	2.38	0.36	9.28	4.47	0.48	29.5
C1	3	83	14	5.95	1.84	0.31	7.1	3.08	0.43	16.2
C2	3	54	43	8.58	4.71	0.55	9.39	7.21	0.77	8.63

V_t denotes volume fraction of total eutectic carbides,
V_{gb} denotes volume fraction of grain boundary eutectic carbides,
F denotes $[\{V_t(\text{zone C}) - V_t(\text{zone B})\}/ V_t(\text{zone C})] \times 100$

Figure 4 reveals microstructures of eutectic carbide skeleton precipitates which have been responsive for long term strengthening effects at high temperature of pyrolysis and cracking of petrochemical products. Results of this investigation have been as follows: (i) Morphologies of as cast primary precipitation have been observed to vary from outer wall to inner wall along radial direction in dendrites and grain boundaries. These precipitations are : (a) thin film carbides, (b) blocky carbides, (c) lamellar carbide clusters resembling pearlite and (d) skeleton carbides. (ii) Increase in cooling rate has increased lengths of columnar grains/dendrites and increasing electromagnetic field has refined grains to cellular morphologies. These have subsequently changed positions of eutectic carbide precipitations from dendrite boundaries to grain boundaries. (iii) Centrifugally cast heat resistant tubes have shown distribution of eutectic carbides which have been related to solute redistribution and growth conditions of pre-solidified γ-grains during solidification. (iv) Introduction of electromagnetic field during solidification has improved creep rupture strength of centrifugally cast heat-resistant 25Cr20Ni steel tubes. This infers that refined grains and subsequent increase in eutectic carbides along grain boundaries have increased creep resistance and has also retarded nucleation and linkages of the creep cavities or cracks. Comparative increase in creep rupture strength has been revealed in figure 5 [12].

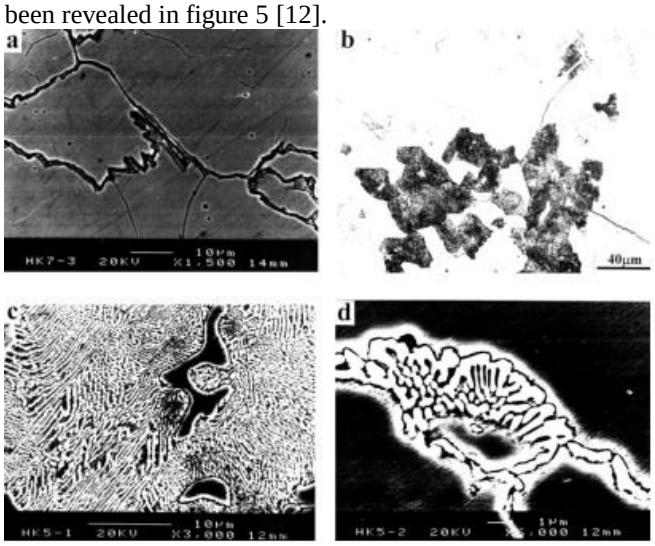

Figure 4: Typical morphologies of the eutectic carbides in the tube (fig. 3), (a) thin film – like carbides in the zone A, (b) morphologies of the eutectic carbides in outer layer of zone B, (c) high magnification of lamellar carbide clusters shown in (b) and (d) the skeleton –like carbides in the zone C [12].

HK40 steels of different microstructures have been investigated by S.J.Zhu [13] to measure creep crack growth behavior at 1144 K on compact tension specimens. More resistance to creep crack growth has been observed to interplay by skeleton-shaped carbides in grain boundaries than blocky-shaped precipitates. Secondary carbides have similar resistance to crack growth however only upto critical size; coarsening above critical size has reverse effect to creep crack growth [13].

Fang Daining Shen Fuzhong [14] has described creep and fracture failure of HK40 furnace tubes at high temperature. Creep crack growth behavior has been evaluated by parametric measurement of high-temperature crack-opening displacement (COD). Suggested equipment and procedure are of general creep test equipment fitted with a long-focusing microscope and derived formula used has relation between crack opening displacement and parametric deformation energy rate for a C-shaped specimen. The experimental data based on tests on C-shaped specimens at 1144 K are correlated by using five mechanical parameters; these are stress intensity factor, net section stress, reference stress, COD rate and deformation energy rate. Better relation has been suggested between creep crack growth data to deformation energy rate and COD rate [14].

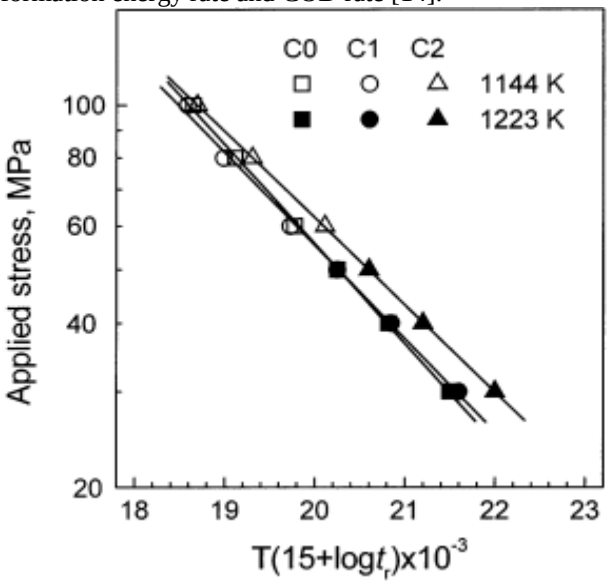

Figure 5: Larson-Miller rupture curves for the centrifugally cast 25Cr20Ni heat-resistant steel tubes [12].

High temperature petrochemical plants widely use centrifugally cast 25Cr-20Ni-0.4C austenitic steels (ACI HK40). Improvement in efficiency of petrochemical industries is achieved by development of improved high strength materials, which has been operated at greater stresses, pressures and temperatures. Structure property correlation studies in HK40 steel clarified and revealed better creep rupture strength [15]. Md Bahaa Zaghloul et al. [15] have clearly described studies on strengthening mechanisms of centrifugally cast HK40 tubes to obtain highest available strength from (i) primary cast structure, (ii) secondary structures inside the grains and (iii) grain boundary conditions. Suitable primary structure has been obtained from control of centrifugal casting conditions, e.g. cooling rates. Secondary structure of precipitations have been obtained from best cast conditions of carbide forming elements during creep rupture tests after addition of carbide forming elements such as Ti and Nb. Resistance to weld cracking at heat affected zones of castings have appeared to improve by dual additions of Ti and Nb. Creep rupture strength has been improved by combined addition of Ti and Nb in HK 40 steels. This has been studied about grain boundary precipitates and their morphology in relation to void formation and crack propagation which have led creep failure. Table 3 has shown about changes in centrifugal tube casting conditions at different cooling conditions e.g. solidification in graphite moulds at slowest cooling rate (477 K /min.) and copper moulds at fastest cooling rates (1077 K/min.) with different chemical compositions. Related structural variations have been shown in table 4 [15].

Table 3: Chemical compositions of HK40 with the cooling rate according to casting condition [15].

Specimen	Casting condition		Cooling rate ^{o}C/min	Chemical compositions, wt.%		
	Mould type	Centrifugal force		C	Ni	Cr
G-7	Graphite	70 g	240	0.35	20.0	24.4
G-10	Graphite	100 g	384	0.36	20.7	24.6
CT-10	Cast iron	100g	636	0.37	20.8	25.0
C-7	Copper	70g	---	0.36	20.3	24.9
C-10	Copper	100g	804	0.35	21.0	24.0

Si: 0.34-0.45, Mn: 1.30-1.44, N: 0.02-0.08, S: 0.01-0.012, P: 0.002-0.003

Table 4: Structural variations and creep rupture strength of HK40 [15].

Specimens	Volume fraction of carbide eutectic (%)	Lattice parameter of as cast (^{o}A)	Dissolved carbon content of as cast (wt.%)	Mean size of dendrite cell (mm)	Creep rupture strength* (kg/mm^2)	
					1000 ^{o}C 100 hr	1000 ^{o}C 10,000 hr
G-7	5.03	3.5945	0.12	0.045	1.50	0.90
G-10	4.31	---	---	0.048	1.55	0.92
CT-10	3.44	3.5958	0.15	0.056	1.60	0.95
C-7	2.09	---	---	0.075	1.70	1.05
C-10	1.99	3.5962	0.17	0.093	1.75	1.15

* creep rupture strength has been calculated from regression equation.

Creep rupture strength of HK40 steel has been enhanced by suitable cast structure through control on cooling rate during solidification. Creep rupture strength has also been controlled by dispersion strengthening from secondary precipitation. Carbide stabilizing elements which have been less soluble in austenite matrix and have induced different carbide morphologies have appeared to improve creep rupture properties. Author has described single element as well as combined addition of Ti and Nb in HK40. Chemical compositions have been shown in table 5a, b and c [15].

Table 5: Chemical compositions of Ti and Nb added HK40 steels [15].

Table 5(a)

Mark	C	Ti
T_1	0.45	0.19
T_2	0.44	0.24
T_3	0.46	0.76
T_4	0.31	1.76

Table 5(b)

Mark	C	Nb
N_1	0.44	1.42
N_2	0.45	1.74
N_3	0.47	1.95
N_4	0.53	3.60

Table 5(c)

Mark	C	Ti	Nb	(Ti+Nb)/C *	Ti/(Ti+Nb) *
K_1	0.43	0.15	0.47	0.23	0.38
K_2	0.44	1.13	1.15	0.97	0.66
K_3	0.45	0.15	0.60	0.26	0.32
K_4	0.45	0.15	1.75	0.58	0.14
K_5	0.43	0.38	0.51	0.63	0.76
K_6	0.46	0.71	1.15	0.71	0.55

Ni: 19.62-20.51, Cr: 24.11-26.37, Si: 1.28-1.73, Mn: 1.29-1.55, * = atomic ratio, Casting condition = Copper mould and force of centrifuge = 100 g.

Control of as cast and secondary structures of steel have been optimized from high temperature strength for centrifugally cast HK40 steel. These have been (i) Highest dendritic growth rate during solidification of centrifugal cast pipes has produced largest dendritic cell structure to produce better creep rupture strength, (ii) Studies of crack propagation from grain boundary morphology after Ti or Nb alloy addition have reproduced (a) formation of discontinuous grain boundaries by carbides during secondary creep by secondary precipitation after Ti addition has delayed crack propagation through grain boundaries during tertiary creep which has enhanced total creep life, (b) Crack propagation in case of Nb alloyed condition has a looped path around and inside lamellar carbide cell boundaries, which has been more slower than Ti added steel. This has suggested that voids or cracks have been less important to reduce creep life. (iii) Addition of both Ti and Nb has improved creep life of HK40 steel at high temperature upto extraordinary extent compared to single addition. Estimated improvement has been 1.7 times to that of plain HK40 steels performing at same temperature and similar in performance to plain HK40 steel at comparatively lower temperature of 373 K.

Increasing importance of extending service life time of centrifugally cast HK40, HP40 and HP-niobium modified reformer tubes used in (i) refining, (ii) petrochemical (iii) fertilizer industries, (iv) radiant catalyst tubes has been traditionally estimated from mathematical models and policies of extrapolation. Life limitation variables have been (i) creep, (ii) combination of internal pressure and Hoop stress and (iii) Through wall thermal stresses generated by operational transients. Mathematical and theoretical models have been normal practice to assess life within process complexities. Irrespective of various destructive test methods, non-destructive methods have been attractive[15].

B.P.Sachs et al.[16] have described mathematical modeling from results of NDT by a software package TUBLIFE computer program. Chronology of NDT has been evaluation of (i) creep damage first develops voids, (ii) coalescence of voids, (iii) microcrack formation, (iv) macrocrack formation, (v) evolution of rupture and (vi) acceleration by service conditions. TUBELIFE has been a probabilistic life assessment software package. This has been a statistical program rather than a deterministic analysis of reformer [16]. Evidences of creep life assessment by microstructure preparation a destructive test method has been reported by Yi Ding et al.[17]. This is analysis of micrographs from HK40 furnace tubes after different service duration. Creep research and residual life assessment has indicated that creep process has been linked to process of carbide aging and precipitation [17]. Microstructure analysis has been referred to be a comparative study for development of new furnace tube material [18].

Wang Fugang et al.[19] have estimated about 20,000 hours more life by plot of Larson-Miller parameter over a furnace tube of HK40 steels which has already served for 42,000 hours. There has been appreciable effect on deterioration of tubes from lower carbon content than standard value of carbon content in reformer tube, e.g. better performance has been found in tubes containing 0.35% carbon than standard HK40 tube containing 0.38% carbon [19].

III. Failure Analysis of HK40 Steels

Failure analysis has been mandatory step in high temperature and pressure implements to assess valuable remaining life

assessment. Life prediction has been proposed by following methods (i) Larson-Miller parameter, (ii) θ-projection method, (iii) Monkman-Grant relationship and (iv) methods based on reliability. Way of life assessment has been extrapolation of curves of stress-rupture tests parallel to material's master curve. Specimens for creep-rupture tests have been selected from zone of tubes which are subjected to relatively serious damage under operating conditions. Periodic tests on heat resistant HK40 steels and generation of data has been referred to accumulate experimental data for analysis of damage evolution in material. Therefore comparative deviation of data trend between virgin (master curve) and service exposed specimen has logical importance. Z-parameter has been considered as indication about magnitude of deterioration in creep rupture strength. Accumulation of damage of HK40 austenitic steels based on confidence level, using Z-parameter method has been applied to evaluate remaining life. Li Xing et al.[20] have described as follows: (i) Z-parameter method has been referred to characterize change in rupture properties for HK40 steel. Expression for non-linear master curve of stress versus Larson-Miller parameter P has been [20]

$$P = 22.692 - 4.51 \log \sigma - 0.0054 \sigma. \quad (4)$$

Therefore family of curves parallel to master curve has been expressed as

$$P = (22.692 - Z) - 4.51 \log \sigma - 0.0054 \sigma, \quad (5)$$

where Z has been magnitude of deviation from master curve. This value has been evidence of deterioration in rupture properties. (ii) Original data of HK40 steel has been well supported by normal distribution of Z-parameter. (iii) Confidence level has been introduced to perform damage evaluation. At a certain service time value of damage accumulation increases with increase in confidence level [20].

IV. Ethylene Cracking Tube

Usual design for normal life of 1,00,000 (11.4 years) hours has been normal practice, for tubes made of cast creep resistant austenitic (26Cr, 35Ni, 0.4C) steel from HP grade. Actually this life varies within 30,000 and 80,000 hours based on the service conditions and quality of materials. Life has been therefore a competing phenomenon among (a) favorable and (b) unfavorable conditions, e.g. (a) design, carefulness, operational uniformity and (b) over heating, stress corrosion cracking, creep and fatigue. Table 6 has shown material specifications and design parameters.

Table 6: Material specification of ethylene cracking tubes of sample and design parameters [21].

Tube material	HP40	
Composition, wt.%	C Si Mn P S Cr Ni Nb W Fe	3.8 0.65 0.31 0.07 0.04 23.4 41.9 1.36 0.80 Balance
Design temperature	973-1173 K	
Tube size	Outer diameter Thickness Length	63 mm 6.4 mm 12 m

Tensile strength of service exposed tube: 317 MPa at 298 K.

Bulged specimen has been shown in figure 6. Figure 6a and 6b have shown local penetration and cross-sectional view respectively. Changes in shape from circular to elliptical are indication of operation at higher temperature than stipulated and for shorter times. Figure 7a has shown penetrated crack with about 2 mm open. Figure 7b has shown to view a crack on tube inner surface. Crack is discontinuous in inner surface. Penetrated crack is longer in outer surface than that in inner surface which indicates that crack has originated from outer surface. Absence of wall thinning and plastic deformation near crack reveals that crack is brittle in nature. Figure 8 is from scanning electron micrographs of bulged penetrated surface. Rupture has been shown intergranular fracture. Oxidation and over heating has changed grain shapes to globular form. Composition of these globular grains has been shown in table 7 after analysis by energy dispersive spectroscopy. Heating effects to outer surface from burners under oxidizing atmosphere has been indicated by presence of more chromium and oxygen in the EDS analysis report of table7.

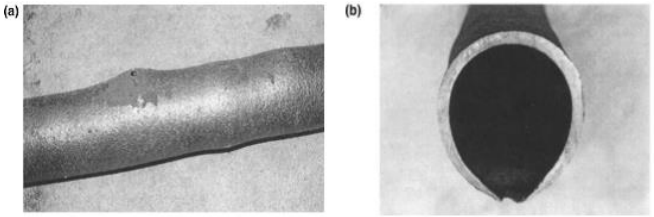

Figure 6: Tube bulge of as received sample, (a) general view and (b) cross-section [21].

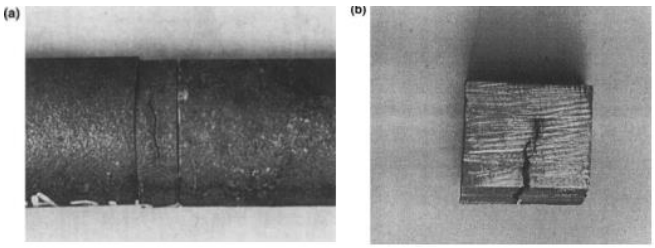

Figure 7: Circumferential crack at (a) outer surface; (b) inner surface [21].

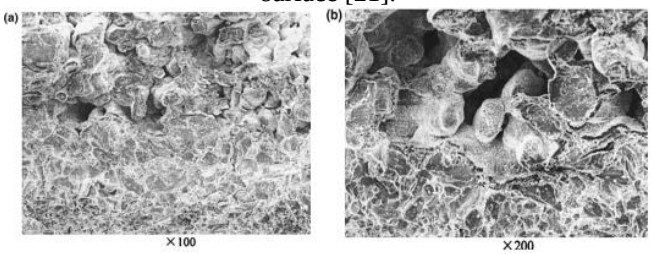

Figure 8: Globular grains due to melting [21].

Table 7: Composition of globular grain by SEM/EDS [21].

Element	Characteristic X-ray line	wt. %	at.%
O	K	39.38	65.46
Na	K	6.73	7.78
S	K	1.47	1.22
Cl	K	0.85	0.64
Cr	K	29.56	15.12
Fe	K	7.07	3.37
Ni	K	13.81	6.25
W	L	1.15	0.17

Fractographs of circumferential cracks have been shown in figure 9. Oxidized surface has shown creep cracks in figure 9a. Figure 9b has shown general view of fracture surface. This fractograph has shown nature of crack propagation to be along precipitates. Causes behind appearance like overloaded fracture in general view of fracture have been explained by ductile and tough nature of matrix adjacent to the precipitates, which has been used by propagating crack in a ductile mode. At room temperature tensile tested fracture surface has been shown in figure 10. These brittle fracture modes have been interpreted by presence of large amounts of precipitates on fracture surface. These precipitates have been brittle and have produced secondary cracks. Kaishu Guan et al. [21] have described failure analysis of tubes that has been caused from overheating of bottom burners. Properties of interest have been microstructure changes and mechanical strength values. Failed zones have shown appreciable growth of carbides precipitates. Globular grains appear in budged zones. Bowing down of tubes have promoted crack formation. Preventions have been suggested (a) to lower bottom burner temperatures to avoid overheating or to decrease peak metal tube temperature, (b) periodic check of tube temperature at critical zones, (c) assurance about temperature values lower than designed temperature [21].

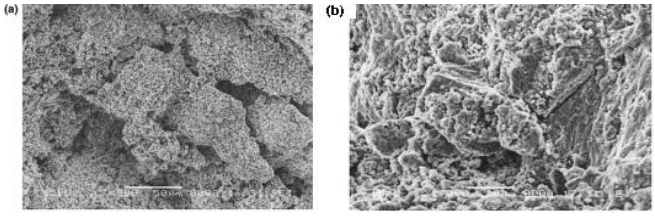

Figure 9: Scanning electron micrographs, (a) general view of creep crack; (b)

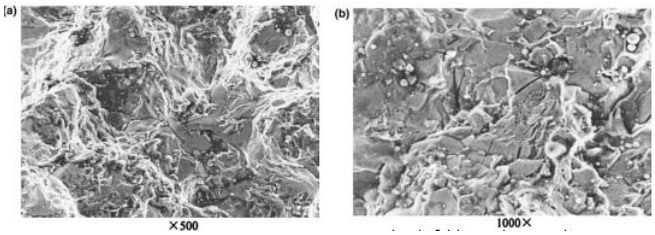

Figure 10: Scanning electron fracture micrographs, (a & b) tensile tested specimens at different magnifications [21].

V. Radiant Tubes of Ethane Pyrolysis Plant

Pyrolysis furnaces in petrochemical plants produce ethylene by cracking ethane (C_2H_6). Mixture of process steam and hydrocarbon gas in 1/3 ratio is passed through coil of reaction tubes, which are externally heated to high temperature. Objective of this processing is to pass low pressure (approaching one atmosphere) gas so as to raise gas temperature (1123 ± 293 K) as quickly as possible and pass it through coil at a high velocity with short residence time (0.72 seconds). Cracking of ethylene produces free carbon (according to reaction: $C_2H_4 \rightarrow CH_4 + C$). Deposition of adherent coke on radiant tube wall from generated carbon has two detrimental effects. They are (i) act of insulation which requires more tube temperature to maintain required gas temperature and (ii) acceleration of carburization attack. Carbon deposition to form coke on inner wall is controlled by cracking of more than 60-65% of ethane. Periodic removal of coke is done by shutting down hydrocarbon feed and passing air and steam through coil. Decoking burns been burnt off some coke and some is blown off after cracking tubes. Severe thermal shock in some local zone induces creep failure where temperature exceeds permissible limits to gradually sag off the tubes. Therefore useful life is dependent on number of decoking cycles based on dictations of process parameters like (i) gas temperature, (ii) flow rate and (iii) conversion ratio. Less decoking cycle on other hand increases rate of carburization attack. Appearance of cracks is found developed in tubes (HP 45 steel and thickness of one centimeter) only after 1/3rd of the useful service life. Figure 11 has shown high density of pores at inner surface of tubes. Inherent defect in centrifugally cast pipes is porosity of bore surface. They have appeared to extend upto 5 mm deep, which has been responsive for continual increase of surface area to enhance carburization attack. Existence of as manufactured pores due to insufficient machining of inner walls has been responsive for adherence of carbon and increase in surface area for carburization. This defect is sometimes referred to be irrecoverable by machining. Figure 18 reveals SEM micrograph and X-ray diffraction analysis of surface scale. Compositions are mostly spinel of tube elements (e.g. $NiFe_2O_4$, $FeCr_2O_4$) [22].

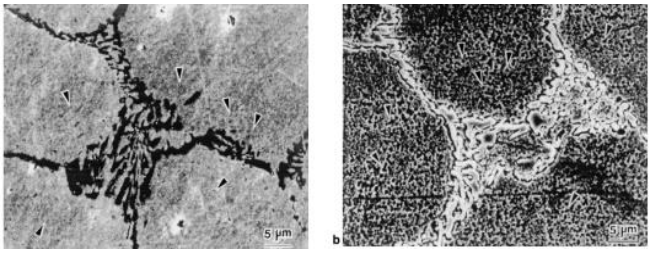

Figure 11: Scanning electron microscopy (SEM) images illustrating porosity in unused tube, (a) as polished and (b) etched sample [22].

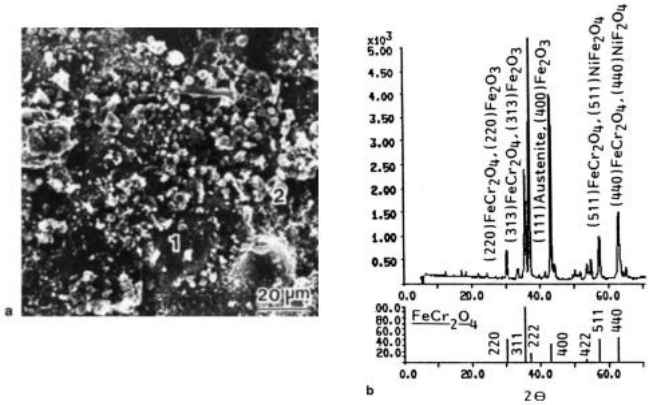

Figure 12: (a) SEM image of scale morphology and (b) XRD pattern derived from surface scale [22].

Cause of this failure of radiant furnace tube is combination of carburization attack and creep attack. Experimental findings have been referred to this case to be consequences of exposure to excessively high temperature during decoking [22].

VI. Fertilizer Plant

Reformer tubes are generally made from cast creep resistant austenitic steel HK grade (25 Cr, 20 Ni, 0.4 C) or HP grade (26 Cr, 35 Ni, 0.4 C). Although the furnace tubes are usually

designed for a normal life of 100,000 h (11.4 years), their actual service life, however, varies from 30,000 to 180,000 h, depending on the service conditions and of course on the quality of materials [23]. Due to prolonged exposure to high temperature, the microstructure of the material is subjected to degradation. For example, in the early stages, precipitation of carbides occurs. Following this, there is reduction in strength and embrittlement due to coalescence and coarsening of the carbides. Further degradation might lead to creep cavitation damage, micro cracking and final propagation of macro-cracks leading to catastrophic failure. Due to this inevitable damage, over the past two decades much research has been done in this area [24-28].

An ammonia and urea complex in a reputed fertilizer plant uses natural gas as feedstock for ammonia production. The natural gas is further reformed with the help of steam in the catalyst tube of the primary reformer. The primary reformer for unit II ammonia plant 1350 T/D of Haldor Topsoe design [29] is a furnace containing 288 catalyst tubes arranged in two radiant chambers of 144 tubes each. The catalyst tubes are vertically installed and supported at the bottom and are free to expand upwards. The feed gas of naphtha, vapors and steam enters at the top end at a temperature of 763 K and pressure of 32 kg/cm^2 and flows down over the catalyst in individual tubes before coming out at 1053 K and at a pressure of 31 kg/cm^2. The reforming reaction takes place in the catalyst tubes and is endothermic. For this, heat is provided by firing a total of 576 burners in the furnace at various elevations. The heat is transferred to the catalyst tubes through radiation and the metal temperature is maintained between 1143 and 1163 K. The material specification and design parameters are given in table 8 (figure 13a) [30].

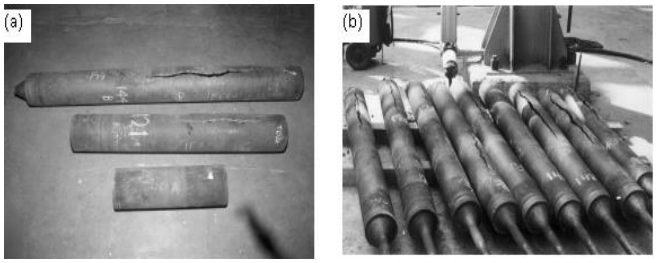

Figure 13: (a) Photograph of as received samples: 144A, 144B, 121;
(b) Photograph of nine failed tubes, as received [30].

Table 8: Material specification and design parameters of reformer tubes [30].

Tube material	HK 40+Nb micro alloy	
Composition (wt.%)	C Si Mn Cr Ni Ti Fe	0.45 1.50 1.00 25.00 35.00 Additions (not disclosed) Balance
Tube size	Outer diameter (OD) Thickness	152 mm 10.7 mm
Design temperature	906 ^{o}C	
Design pressure	34 kg/cm^2	

At the time of failure the reformer was being started up with only 60 burners firing in the reformer. The gas in the catalyst tubes was mainly hydrogen and steam at a pressure of 3 kg/cm^2 only. A total of seven tubes ruptured in the bottom portion in one corner of the radiant chamber. Another two tubes ruptured away from this zone in the bottom portion. The rupture was longitudinal. These tubes had been in operation for 2 years. Dimensional measurements of the failed reformer tubes are shown in table 9 (figure 13b).

Table 9 Dimensional measurement of the failed reformer tubes and their measured crack lengths [30].

Tube no.	Crack length (mm)	Max. OD (mm	Crack length (mm)	L (mm)a	Pig tail diameter (mm)
144	850	169	19	470	42.4
143	570	160.7	12.4	625	42.4
142	880	159	16	870	42.5
141	630	158	17	860	42.1
140	620	158.6	13	870	42.2
139	630	157.4	10	280	42.2
138	500	156.9	11.5	1220	42.2
131	400	154.9	10	1100	42.2
121	600	155.2	---		42.1

The failed tubes were replaced with new tubes and the pressure drop in each tube was measured. The pressure drop in the case of tube No. 121 was found to be excessive. The pigtail corresponding to this tube was cut open and choking due to damaged catalyst was observed.

Chances of steam/water entrapment in the tube were explored. It was found that possibility of water entrapment is small because during shutdown, nitrogen is passed through all the tubes at 6 kg/cm^2 for 24 h.

Temperature in the radiant zone where seven tubes numbering 138–144 had failed was reported to be very high as was observed by the plant engineers soon after the failure of the tubes.

The possibility of hydrogen coming out of the leaked tube cannot be ruled out.

Details regarding firing of the number of burners (out of 60) in the bottom zone where failure had occurred were not available.

The failure of the tubes was caused by overheating arising out of choking caused by damaged catalyst. To avoid such choking, precautions should be taken while charging the catalyst that no broken piece of catalyst or any external material goes along. Nitrogen which is used for cooling down the tubes and which was retained inside during idle periods should be dry enough. Overheating during service is primarily responsible for significant degradation in mechanical properties and microstructures in the bottom portion of tube no. 144B of the reformer tubes [30].

VII. Petrochemical Industries

Jian-Ming Gong et al.[31] have defined reformer tube as key component used to produce hydrogen-rich gas from a mixture of hydrocarbons and steam at high temperature. Designed life of furnace tubes have been nominal life of 1,00,000 hours. This has been recommended Practice 530 from American Petroleum Institute (API). Depending on quality of material and service conditions actual service life varies from 30,000 to 1,80,000 hours. Centrifugal cast creep resistant austenitic

steel of HK and HP grade applicable for this purpose has been degraded by carbide precipitation, coarsening coalescence, related embrittlement and reduction in strength in service exposure. Trend of degradation has been illustrated by creep cavity formation, cavity coalescence, micro-cracking and propagation of micro-cracks. Traditional studies are for crack zones and replacement of whole tubes. In this case authors have experimental investigations of whole tube for damage and remaining life assessment and requirements of maintenance. Table 10 has described about arrangement of tube and arguments of interest. Dissimilar metal welding (DMW) joints have been made at two ends between Cr5Mo and HK40 steels without post-weld heat-treatments, whereas whole furnace tube has been fabricated by welding four to five short tubes by three to four similar metal welds [31].

Table 10: Microstructure and effective wall temperature [31].

Locations	Parent metal	Weld metal	Effective wall temperature
Top end flange and dissimilar metal weld	Little change of carbide morphology has been observed. Normal carbides have been well framed in dendritic grain boundaries or between boundaries	Primary carbides have been precipitated along boundaries while secondary carbides have been dispersed in austenite matrix.	< 773 K
Weldment from top to bottom	Primary carbides precipitated along boundaries while secondary carbides have been dispersed near grain boundaries	Primary carbides have been linked and coarsening while secondary carbides have been dispersed near grain boundaries	923-973 K, slight carburization has been found on inner surface of tube.
	Primary carbides has been linked and few of them have been blocky while secondary carbides have been dispersed inside grain and tend to coalesce	Primary carbides have been linked have been coarsening while secondary carbides coalesce obviously inside grain	1053-1073 K
	Primary carbides have been linked and few of them have been blocky while secondary carbides have been dispersed and coalesce obviously inside grain	Primary carbides have been linked and blocky while secondary carbides have been almost dissolved. In HAZ intergranular microcracks have been observed in inner surface	1123 K
Parent metal located in center of two tube sections in middle part of whole weld	Primary carbides have been linked while secondary carbides have been dispersed and tend to coalesce inside grain. The sigma-phase appears inside grain		1123 K The sigma-phase implies that location had been a skin temperature above 1073 K.
	Primary carbides have been linked and few of them have been blocky while secondary carbides coalesce obviously inside grain. Material deterioration has been more severe than previous case		1143 K
Most bottom weldment	Primary carbides have been linked and blocky while secondary carbides coalesce obviously and have been partly dissolved. SEM observation reveals that there have been strings of cavities and few microcracks in inner surface of tube (figure 14a)	Primary carbides have been significantly coarsening and blocky while secondary carbides coalesce obviously and have been partly dissolved	1143 K From inner surface to middle of tube there have been strings of cavities and some microcracks (figure 14b)
Bottom end flange and dissimilar metal weld	Primary carbides precipitated along boundaries while dispersed secondary carbides tend to coalesce near grain boundaries	Single distributed cavities have been found in grain boundaries	753 K

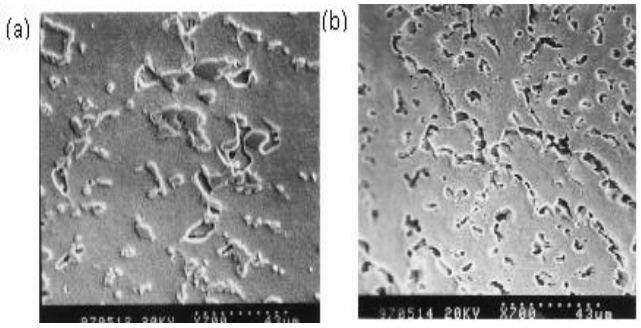

Figure 14: (a) Grain boundary creep voids near inner surface in base material (SEM, ×700) and (b) Grain boundary creep voids and microcracks in weldment (SEM, ×700) [31].

Damage analysis of reformer tube exposed for ten years has been done by metallographic analysis. Damage level ranks have been related to remaining life assessment. Numerical simulation has been done to assess development of damage and distribution along whole reformer tube. Authors have suggested following descriptions. (a) Carbides in this case have been treated as damage of tubes after illustration as zones of preference for cavitations defects, e.g. grain boundary carbides. (b) Welds have been treated as weakest link detrimental to useful service life. (c) Further arguments are that carbides have not been rate controlling because of variation in damage between comparatively more damage in lower parts than upper parts, however similarities in metallographic results and results of finite element method (FEM) has been in accordance. Therefore life management from damage theory has not been accepted as sufficient. (d) Consideration of maintenance plan based on scientific understanding of creep behavior between lower and upper part has referred to replacement of lower part of reformer tubes based on reach of safe rupture life [31].

Antonello Alvino et al.[32] have been describing reformer furnaces to use in petrochemical industry for large scale production of hydrogen by catalytic reaction between hydrocarbons and steam. Radiant columns consisting of tubes filled with catalyst and continuously heated up to an operating temperature exceeding 1073 K have been conducted to produce these endothermic reactions. Increased production and efficiency has been referred to improve (i) for steam to hydrocarbon ratio of 3:1, and higher operating (ii) temperature and (iii) pressure simultaneously. Authors have described premature failure in centrifugally cast HP grade steels from damage mechanisms like (i) creep, (ii) carburization, (iii) oxidation, (iv) thermal shock, (v) over heating as described by previous authors. Subsequent defects have been (vi) unfavorable chemical reactions under certain conditions, (vii) carbon depositions at internal surfaces of catalyst tubes, (viii) extra more deformation of tubes to reduce heat dissipation in between columns, (ix) thereby leading to hot spot formation in material, (x) macroscopic deformation of cross section at lower portion of columns subjected to higher thermal gradients, and (xi) tube ovalization. Author has described comparative damage assessment and life prediction of two tubes from two furnaces as follows in table 11 to table 14. Etchants used for microstructure preparation, Murakami's reagent: 10 g $K_3Fe(CN)_6$, 10 g KOH, 100 ml H_2O or Groesbeck's reagent: 4 g $KMnO_4$, 4 g NaOH, 100 ml H_2O [32].

Table 11: Design data of two plants [32].

Features in furnace	Furnace under 8 years of service exposure (F01)	Furnace under 9 years of service exposure (F02)
Typology	Top firing	Top firing
Number of burners	60 arranged on 5 rows	60:36 inners and 24 outers
Feed gas composition	Light benzene sulphur-free (70%) + GPL sulphur-free (30%)	Fuel gas (80%) + GPL or methane (20%)
Number of catalyst tubes	204 tubes arranged on 4 rows	176 tubes arranged on 4 rows
Tube dimensions	OD 128.3 mm	OD tubes arranged on 4 rows
	ID 101.6 mm	ID 101.6 mm
Tube service pressure	30 bar	25 + 27 bar
Maximum tube design pressure	33 bar	32.7 bar
Tube service temperature (top)	803 K	Max. 833 K
Tube service temperature (bottom)	Max. 1133 K	Max. 1153 K
Maximum tube service skin temperature	1163 K	1163 K
Maximum tube design skin temperature	1228 K	1223 K
Hydrogen production	61.000 Nm^3/h	42.000 Nm^3/h
Operating service life	85,000 hours	96,000 hours

Table 12: Chemical composition of analyzed alloys [32].

	C	Si	Mn	Cr	Ni	Nb	Ti	Cu	Fe
F01	0.40	1.50	1.50	25.00	35.00	1.50	--	--	Bal.
F02	0.43	1.40	1.00	25.00	35.00	1.50	Vare.[a]	0.25	Bal.

Proprietary addition: % Ti ranges from 0.05 to 0.30.

Table 13: Vickers hardness values from test results performed on the supplied materials [32].

Sample	Upper				Lower			
Tube	Outer wall	Bulk 1	Bulk 2	Inner wall	Outer wall	Bulk 1	Bulk 2	Inner wall
F01	211 ±8	217±9	216±8	243±10	215±6	212±3	217±7	252±5
F02	172±10	170±10	167±10	181±5	172±5	163±7	162±6	175±10

Table 14: Ultimate tensile strength values from test results performed at room temperature on supplied materials. For reference materials, data supplied by manufacturer have been used [32].

Sample tube	Upper	Lower
F01	294 ± 15	267 ± 5
F02	320 ± 22	175 ± 10
Reference		
G 4852	470	
G 4852 micro	470	

Interpretations of degradation in these cases show appreciable loss in ductility, increase in hardness and correlated respective microstructures and evidence of voids, cavities and crack damage by creep deformation. Comparative damage between F01 (more) and F02 (less) are due to presence of Ti in F02 tube, variation in chemical reaction strategy, temperature, pressure, chemical composition of fuel gases, steam/hydrocarbon ratio, variation in process parameters and thereby influence to early damage and aging and different decoking strategy to promote coking effects more for F01 tube (figure 15) [32].

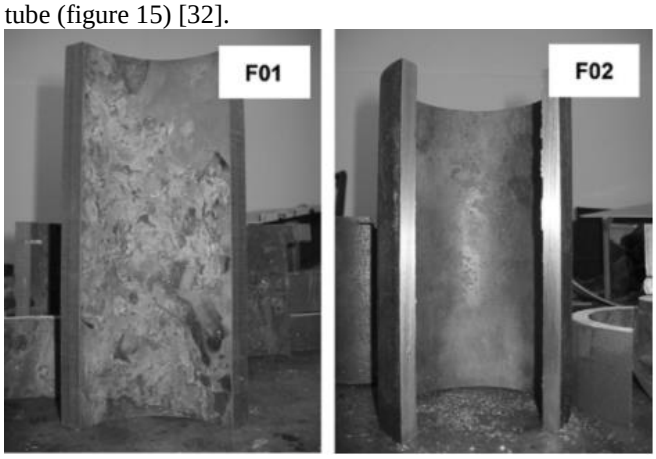

Figure 15: Photographs of reformer tubes F01 and F02 [32].

VIII. Ammonia and methanol plant

Defects in weld joints between HK40 and SS 321 have been characterized by S.K.Bhaumik et al.[33]. for ammonia and methanol plant. Steam reforming of hydrocarbon at high temperature and pressure produces CO, CO_2 and H_2. Formation of corrosive gasses in processing are fluorine, hydrofluorosilicic acid, SO_2 and SO_3 gas and NO_x gas, acid mists, etc. failure in ammonia plant are mostly because of corrosion of these gases. These corrosion processes have been encountered to be uniform corrosion, galvanic corrosion, intergranular corrosion, stress corrosion, cavitation, fretting corrosion, high temperature corrosion, hydrogen embrittlement, metal dusting, etc. This has reported that even after caution by different ways like selection of material, fabrication techniques, design of plants, etc this defect has remained irrecoverable. Reformers of plant has been important portion, its failures have been responsive for premature shut downs, and associated losses in terms of damages to equipments, production losses, and safety hazards, etc. Analysis of such case has been described by failure from stress corrosion cracking of in-situ sensitization of heat affected zones (HAZ) in weld joints. This has been accounted a failure from improper filler rod at dissimilar weld joints between stain less steels and mild steels. Traces of chlorides and alkali are treated as corrosive constituent in process gases for HAZ however these corrodants have been affectless for SS321 and HK40 steels. This has been effectible after in-situ sensitization of zones in preference [33].

IX. Fertilizer industries

Referred chemical reactions of ammonia synthesis for urea production in fertilizer industries are used inlet process gases at temperatures of 723-773 K and at outlet manifold to be 1073-1173 K under pressures of 1-4 MPa. Tube alloys used are IN519, HP-Nb modified and HP-W modified. In service there are variations in temperature and thermal load distribution along different sections of tube. Factor behind such variations are (i) burner regulation, (ii) loss in catalyst activity, (iii) aging of catalyst, (iv) Collapse of catalyst column inside tube [34-36], (v) creep of tube material, (vi) thermal shock, (vii) overheating and (viii) carburization of inner wall. Therefore as designed life of 11.4 years or 1,00,000 hours appears to vary between 3 to 15 years [37-39]. Failure investigation of HP-microalloyed tube shows circumferential cracks on inner wall side. These have been creep damage after exposure to high temperature in preference. Weld is treated as the weakest link to crack at isolated cavities in the base metal. In between inner wall and mid-thickness zones these cavities are present in preference. No creep voids are found in outer wall zones. HAZ regions are zones of preference for longitudinal cracks. Annealing to re-weld and rejuvenate the old tubes are more detrimental to the cavities than morphological variation in carbide from heat-treatment effects compared to prior existing carbides [40-42].

X. Conclusion

Extrapolated reformer tube life assessment after laboratory scale experiments have been traditionally done by stress/accelerated creep rupture tests and creep tests. Microstructural inspection revealing creep cavitations are zones of voids formed adjacent to coarsened carbides, carbides at grain boundaries, or as solidified blow holes/ pin holes of centrifuge. Carbide precipitation, re-dissolution and further re-precipitation have been strategies of alloy elements to increase strength, to increase ductility and further re-strengthening with precipitate free zones of more ductility respectively.

References

[1] S. A. Jenabali Jahromi and M. Naghikhani: Failure Analysis of HP40-Nb Modified Primary reformer Tube of Ammonia Plant, Iranian Journal of Science & Technology, Transaction B, 28 (B2) (2004) 269-271.

[2] Remaining life assessment and failure analysis of service exposed reformer tubes, (SSP-9339) sponsored by Indo-gulf Fertilizers, CSIR-National Metallurgical Laboratory, Jamshedpur, India, 2009.

[3] D.Knowles, K.Buchanan and M.Kral: Condition assessment strategies in centrifugal cast HP steam reformer tube alloys, in: ECCC creep Conference, 21-23 April, Zurich, 2009.

[4] J.M.Gong, S.T.Tu and K.B.Yoon: Damage assessment and maintenance strategy of hydrogen reformer furnace tubes, Eng. Fail. Anal., 6 (1999) 143-153.

[5] C. Maharaj, C.A.C.Imbert and J.Dear: Eng. Fail. Anal., 15 (2008) 1076-1087.

[6] R.Voicu, J.Lacaze, E.Andrieu, D.Poquillion, and J.Furtodo: Mater. Sci. & Eng., A550-551 (2009) 185-189.
[7] R.Vishwanathan, R.Dooley and A.Saxena: [Proc. Conf.], Proceedings of International conference on life assessment and extension, vol.II, Congress centre. The Hague/The Natherlands, 13-15 June, (1988). 175.
[8] P.P.Psyllaki, G.Pantazopoulos and H.Lefakis: Eng. Fail. Anal., 16 (2009) 1420-1431.
[9] G.Pantazopoulos and A.Vazdirvanidis: Eng. Fail. Anal., 16 (2009) 1623-11630.
[10] NRIM creep data sheet no.38A, Data sheets on the elevated temperature properties of centrifugally cast tubes and cast blocks of 25Cr 35Ni 0.4C steel for reformer furnaces (SCH 24).
[11] Ashok Kumar Ray, Sudheer Kumar, Gugulath Krishna, Manoj Gunjan, B.Goswami and Samir Chandra Bose: Microstructural studies and remnant life assessment of eleven years service exposure reformer tube, Material Science and Engineering, A529 (2011) 102-112.
[12] X.Q Wu, H.M Jing, Y.G Zheng, Z.M Yao, W Ke and Z.Q Hu: The eutectic carbides and creep rupture strength of 25Cr20Ni heat-resistant steel tubes centrifugally cast with different solidification conditions, Materials Science and Engineering: A, 293 (1–2) (2000) 252–260.
[13] S. J. Zhu, J. Zhao and F. G. Wang: Creep crack growth of HK40 steel: Microstructural effects, Metallurgical Transactions A, 21(6) (1990) 2237-2241.
[14] Fang Daining and Shen Fuzhong: Research on Creep Crack Growth of HK—40 Alloy with High—Temperature COD, Journal of Nanjing University of Technology (Natural Science Edition) 1987-01.
[15] Md. Bahaa Zaghloul, Takayuki Shinoda, and Ryohei Tanaka: On The Strengthening of the centrifugally cast Hk40 tube, Metallugical Engineering Dept., Tokyo Institute of Technology, Ohokayama, Meguro-ku, Tokyo, Japan, 152, 265-274.
[16] B.P.Sachs, Pecić, Vladimir; Mateša and Branko: Characterization of errors during strengthen off processing furnace tubes status, Welding in the world (0043-2288) 51 (2007); 497-508.
[17] Ding Yi, Shen Fu Zhong and L Yong: Microstructure Analysis on HK-40 Furnace Tubes of Different Service Duration; (Nanjing University of Chemical Technology, Nanjing 210009, China), Materials for Mechanical Engineering; 2002 -07; ©2006 Tsinghua Tongfang Knowledge Network Technology Co., Ltd. (Beijing) (TTKN).
[18] Che Jun-tie and LI Yu-zhu: Microstructure Change and Its Effect on Properties of HK40 and HP40 Furnace Tube; (Beijing Institute of Petrochemical Technology, Beijing 102617, China); Industrial Furnace, ©2006 Tsinghua Tongfang Knowledge Network Technology Co., Ltd.(Beijing) (TTKN).
[19] Wang Fugang, Xu Shanguo, Wang Lai, Quan Renzhe, Wang Huanting and Cao Zhiben: On Structures and Mechanical Properties of the HK40 Steel Tube after 42,000 Hours Operating and Its Residual Life Prediction, Elevated Temperature Furnace Tube Research Group.
[20] Li Xing, Jie Zhao, Fu-zhong Shen and Wei Feng: Reliability analysis and life prediction of HK40 steel during high-temperature exposure, Int. J. of Pressure Vessels and piping, 83 (2006) 730-735.
[21] Kaishu Guan, Hong Xu and Zhiwen Wang: Analysis of failed ethylene cracking tubes, Eng. Fail. Anal. 12 (2005) 420–431.
[22] Anwar UI-Hamid, Hani M. Tawancy, Abdul-Rashid I. Mohammed and Nureddin M. Abbas: Failure analysis of furnace radiant tubes exposed to excessive temperature, Eng. Fail. Anal. 13 (2006) 1005–1021.
[23] American Petrochemical Institute; Calculation of heater-tube thickness in petroleum refineries: API recommended practice 530. 3rd ed. Washington (DC): API; 1983.
[24] Wang Y-L, Shen F-Z and Tu S-T.: Study of crack propagation of HK 40 furnace tubes with C-shaped. Engineering Fracture Mechanics; 47 (1999) 39–47.
[25] S.Konosu, T.Koshimizu, T.Lijima and K.Maeda. Evaluation of creep-fatigue damage interaction in HK 40 alloy. Journal of Mechanical Design, Trans, ASME; 115 (1993) 41–46.
[26] Shipley DG. Creep damage in reformer tubes. Int J Press Ves Piping; 14 (1983) 21–34.
[27] I. May Lke, T.C.da Silveria and C.H.Vianma. Criteria for the evaluation of damage and remaining life in reformer furnace tubes. Int J. Press Ves Piping; 66 (1/3) (1996) 233–241.
[28] J.M.Gong, S.T.Tu and K.B.Yoon. Damage assessment and maintenance strategy of hydrogen reformer furnace tubes. Engineering Failure Analysis; 6(3) (1999)143–153.
[29] S.K.Sinha, S.Chaudhuri, A.K.Ray, J.Swaminathan and R.Singh: Failure analysis of failed reformer tubes samples. Project report no. CIEP (SSP)/2000/0096.
[30] Ashok Kumar Ray, Samarendra Kumar Sinha, Yogendea Nath Tiwary, Jagammathan Swaminathan, Goutam Das, Satyabrata Chaudhury and Ragnubir Singh: Analysis of failed reformer tube, Engineering Failure Analysis, 10 (2003) 351-362.
[31] Jian-Ming Gong, han-Tung Tu and Kee-Bong Yoon: Damage assessment and maintenance strategy of hydrogen reformer furnace tubes, Engineering Failure Analysis, 6 (1999) 143-153.
[32] Antonello Alvino, Daniela Lega, Francesco Giacobbe, Vittorio Mazzocchi and Antonio Rinaldi: Damage characterization in two reformer heater tubes after nearly 10 years of service at different operative and maintenance conditions; Engineering Failure Analysis;(In press) Journal homepage: www.elsevier.com/locate/engfailanal.
[33] S.K.Bhaumik, R.Rangaraju, M.A.Parameswara, T.A.Bhaskaran, M.A.Venkataswamy, A.C.Raghuram and R.V.Krishna: Failure of reformer tube of an ammonia plant, Engineering Failure Analysis, 9 (2002) 553-561.
[34] I.Le May: in Comprehensive Structural integrity (eds) I.Milne, R.O.Ritche and B.Karihaloo, Vol.1 Structural integrity assessment examples and case studies (Eds.) I.Milne, R.O.Ricchie and B.Karihaloo, Elsedier Pergamon (2003) 125.
[35] I.Le May, T.L.de silveria. and C.H.Vianna., Int. J. Pres. Ves. & Piping, 66 (1996) 233.
[36] T.L.De Silveria. and I.Le ay: Int. J. Pres. Ves. & Piping, 119 (1997) 423.
[37] Kaisu Guan, Hong Xu and Zhiwen wang, Nuclear ngg. And Design, 235 (2005) 1447.
[38] E.A.Kenik., P.J.Maziasz, R.W.Swindeman, J. Cervenka and D.May, Scripta Mater., 49 (2003) 117.
[39] A.F.Ribeiro, L.H.De Almeida, D.S.dos Santos.,D. Fruchart. and G.S.Bobrovnitchii: J. of Alloys and Compounds, (2003) 219.
[40] Julian Rodriquez, Sergio haro, Abraham Velasco and Rafel Colas, Materials Charac., 45 (2000) 25.
[41] Gloria Dulce de Almeida Soares, Luiz Henrique de almeida, Tito Luiz da silveria and Iain Le May, Mater. Chrac., 29 (1992) 387.
[42] J.Swaminathan, Raghubir Singh, Swapan Kumar Das and Goutam Das: Failure analysis of weelded reformer tubes of a fertilizer unit, [Proc. Conf.], Proc. Of the Int. Conf. & Exibition on Pressure Vessels and Piping, "OPE 2006 – CHENNAI", 7-9, Feb. 2006, Chennai, India, B10-7 to B10-7.